Critical behavior in the dielectric properties of random self-similar composites

Kunal Ghosh
Department of Physics and Atmospheric Sciences, Jackson State University, Jackson, Mississippi 39217

Ronald Fuchs
Ames Laboratory and Department of Physics and Astronomy, Iowa State University, Ames, Iowa 50011
(Received 20 March 1991)

A theory for the dielectric properties of self-similar composite media is presented, in which inclusions of one component are introduced recursively into a second component. The spectral-representation formalism, which gives a material-independent description of the recursive process, is used. General expressions are derived for critical exponents that describe the behavior of the dc conductivity, the static dielectric constant, and limits of the spectral function near the percolation threshold. The critical exponents depend on the form of the average dielectric function used at each stage of the recursive procedure. The Maxwell-Garnett and Bruggeman forms of this average dielectric function are chosen as examples. Applications of the theory to some dielectric properties of brine-filled porous rocks are discussed.

I. INTRODUCTION

There has been long-standing interest in the problem of deriving dielectric properties of a mixture from those of the individual components. Well-known theories for the average dielectric function are like those of Bruggeman and Maxwell-Garnett; these theories have been used extensively (for a review, see Ref. 1), but the systems to which they are applicable are limited.

Recently there have been many theoretical studies on the dielectric properties of porous systems; however, correct modeling of these continuous systems has been difficult. In trying to explain the dielectric properties of petroleum-bearing rocks, Sen, Scala, and Cohen,[2,3] Mendelson and Cohen (with corrections by Sen),[4,5] Sheng and Callegari,[6] and Sheng,[7] have used approaches based on geometric modeling and effective-medium theories. Lysne[8] and Korringa[9] have given theories to explain the ac response of a mixture. Halperin, Feng, and Sen[10] and Sen, Roberts, and Halperin[11] have used a scaling analysis to estimate the critical exponents for the electrical conductivity, elastic constants, and fluid permeability near the percolation threshold of a class of disordered continuum systems. A review of the properties of porous media and theoretical efforts to explain them can be found in Refs. 12 and 13.

A different approach to explaining the dielectric properties of porous media, based on the spectral representation,[14–16] was adopted by Stroud, Milton, and De.[17] A more general theory was given by Ghosh and Fuchs;[18] it was shown that scaling, similar to that exhibited by discrete systems, occurred in porous rocks.

Computer experiments to simulate random composites have been done mainly on discrete systems. The geometrical properties and dielectric response of random resistor networks (RRN), made up of a mixture of conducting and insulating lattice sites and/or lattice bonds, have been the object of continuous study. For reviews, see Refs. 19–22, and for a collection of articles on the state of the art, see Refs. 23–25. Additional material on disordered systems and their dielectric properties has appeared in the conference proceedings mentioned in Refs. 26 and 27.

These computer experiments on discrete random composites reveal several kinds of critical behavior and associated critical exponents. Some quantities with critical behavior, such as the correlation length, are geometrical, while others, such as the electrical conductivity, are related to transport phenomena. Most of the geometrical exponents have been related among each other through scaling and hyperscaling laws, and there has been some progress on finding relations between critical exponents for transport and geometrical properties.[20,28–32]

In this paper we study the dielectric properties of a two-component random composite system in which inclusions of one component are introduced recursively on larger and larger scales into a second component. The theory is a generalization of differential effective-medium theory (DEMT), which was proposed by Bruggeman.[33] In DEMT an infinitesimal fraction of the first component is introduced at each stage, whereas in our theory this fraction can be finite. In addition, we allow an arbitrary mixture equation, which gives the average dielectric function at each stage of the recursive procedure, as well as an arbitrary dimensionality of the space.

The paper is organized as follows: In Sec. II the recursive procedure is described and the spectral representation for the average dielectric function is introduced. This representation allows us to define the form of the mixture equation used at each stage of the recursive procedure in a completely general way which depends only on geometry and is independent of the dielectric functions of the two components. Section III shows how the new spectral function at each stage can be calculated by a

one-dimensional map. A geometrical construction is described which allows the changes in the spectral function to be visualized. In Sec. IV critical exponents for the dc conductivity, static dielectric constant, and upper and lower limits of the spectral function are defined, and general expressions for these exponents are derived. The critical exponents are calculated for two simple stagewise mixture equations: Maxwell-Garnett theory and Bruggeman effective-medium theory. In Sec. V applications of the theory to dielectric properties of brine-filled porous rocks are discussed briefly.

II. AVERAGE DIELECTRIC FUNCTION OF COMPOSITE

A. Recursive construction of system

In the proposed recursive construction, we start with pure component 2 and randomly make holes, filled with component 1, with filling fraction f_1. This is the end of the first stage, as shown in the left-hand panel of Fig. 1. The holes can have different sizes and shapes, and the dimensionality d of the system is arbitrary. However, for simplicity the figure shows the holes as two-dimensional spheres (circles) of the same size. We assume that the hole regions are not connected. At the end of this first stage, the average dielectric function $\epsilon_m^{(1)}$ of the composite depends on f_1 and the dielectric functions ϵ_1 and ϵ_2 of the two components,

$$\epsilon_m^{(1)}=M(\epsilon_1,\epsilon_2,f_1)\ , \tag{2.1}$$

where the form of the function M depends on the geometry of the composite.

In stage 2 of the recursive construction, shown in the right-hand panel of Fig. 1, larger holes are made with the same filling fraction f_1 in the composite medium and are again filled with component 1. Stages 1 and 2 are self-similar in the sense that the geometry of the larger holes in a box of side L' in stage 2 is similar, on the average, so that of the smaller holes in a box of side L in stage 1. The

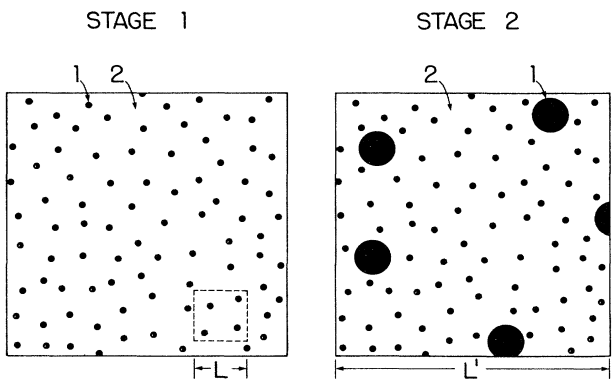

FIG. 1. First two stages in the construction of the self-similar composite medium. Characteristic lengths L and L' for stages 1 and 2 are shown.

average dielectric function $\epsilon_m^{(2)}$ at the end of stage 2 is then given by the same mixture function M as in stage 1, with the dielectric function of the "host" medium 2 set equal to the average dielectric function $\epsilon_m^{(1)}$:

$$\epsilon_m^{(2)}=M(\epsilon_1,\epsilon_m^{(1)},f_1)\ . \tag{2.2}$$

If the same construction is repeated recursively, the average dielectric function at the end of stage j is

$$\epsilon_m^{(j)}=M(\epsilon_1,\epsilon_m^{(j-1)},f_1)\ . \tag{2.3}$$

In writing Eqs. (2.2) and (2.3), we have assumed that, at each stage, the host medium (the medium surrounding the holes formed at that stage) is effectively homogeneous. This implies that the average size of the holes in a given stage should be at least as large as the average distance between the holes in the preceding stage.

The quantities f_1 and $f_2=1-f_1$ are the fixed filling fractions used at each stage of the recursive construction. We shall use $\phi_1^{(j)}$ and $\phi_2^{(j)}$ to denote the actual filling fractions of components 1 and 2 at the end of stage j. Since the actual filling fraction of component 2 is multiplied by f_2 at each stage, we have

$$\phi_2^{(j)}=(f_2)^j=(1-f_1)^j\ , \tag{2.4a}$$

$$\phi_1^{(j)}=1-(f_2)^j=1-(1-f_1)^j\ . \tag{2.4b}$$

Equation (2.4b) shows that, even for a small initial filling fraction f_1 of holes, the hole component 1 will eventually fill space as the iteration proceeds: $\lim_{j\to\infty}\phi_1^{(j)}=1$.

B. Spectral representation

If the function M in Eqs. (2.1)–(2.3) is known explicitly, as, for example, in Maxwell-Garnett theory[34] (MGT) or Bruggeman symmetric effective-medium theory[33] (EMT), the average dielectric function $\epsilon_m^{(j)}$ at the end of stage j can be found by the iterative procedure described by these equations, for given values of ϵ_1, ϵ_2, and f_1. However, it is more useful to describe this iterative procedure using the Bergman spectral representation,[14] which must be valid for any composite system, even if the mixture function is not known explicitly. This representation contains a spectral function and percolation strengths, which convey the essential information about the geometry of the system at any stage of the recursive procedure, without using specific values of ϵ_1 and ϵ_2.

The spectral representation for Eq. (2.1), which gives the average dielectric function at the end of stage 1, can be written in two alternative forms:

$$\frac{\epsilon_m^{(1)}}{\epsilon_2}-1=f_1\left[C_1\left[\frac{\epsilon_1}{\epsilon_2}-1\right]+\int_0^1\frac{G_1(n)}{(\epsilon_1/\epsilon_2-1)^{-1}+n}dn\right]\ , \tag{2.5}$$

$$\frac{\epsilon_m^{(1)}}{\epsilon_1}-1=f_2\left[C_2\left[\frac{\epsilon_2}{\epsilon_1}-1\right]+\int_0^1\frac{G_2(n)}{(\epsilon_2/\epsilon_1-1)^{-1}+n}dn\right]\ , \tag{2.6}$$

where $f_1+f_2=1$. Here C_1 and C_2 are known as the percolation strengths of media 1 and 2, respectively, whereas $G_1(n)$ and $G_2(n)$ are the spectral functions, defined for $0<n<1$. The percolation strengths must lie in the range (0,1), and the spectral functions are non-negative.

The spectral function $G_1(n)$ is closely related to the surface-mode spectrum in frequency regions where $\mathrm{Re}(\epsilon_1/\epsilon_2)<0$. To show this relation, let component 1 be a free-electron metal described by the Drude dielectric function $\epsilon_1=1-\omega_p^2/\omega(\omega+i\gamma)$, where ω_p is the bulk-plasma frequency and γ is the electron-scattering rate, and let component 2, which we consider as a host, be vacuum ($\epsilon_2=1$). Then the denominator of the integrand in Eq. (2.5) is $-\omega(\omega+i\gamma)/\omega_p^2+n$. Suppose that $G_1(n)$ has a peak at $n=n_0'$: $G_1(n)=A\delta(n-n_0')$. Then the integral in Eq. (2.5) reduces to $A/[n_0'-\omega(\omega+i\gamma)/\omega_p^2]$, and there will be an absorption peak, i.e., a peak in $\mathrm{Im}[\epsilon_m^{(1)}(\omega)]$, of width $\Delta\omega\sim\gamma\omega_p$ and area proportional to A centered at the frequency $\omega_1=\sqrt{n_0'}\,\omega_p$. The spectral function for Maxwell-Garnett theory, which applies to a dilute system of spherical particles, is $G_1(n)=\delta(n-n_0')$ with $n_0'=(1-f_1)/3$. Hence there is a corresponding absorption peak at $\omega_0'=\sqrt{(1-f_1)/3}\,\omega_p$, the well-known Mie resonance, corresponding to the dipole surface mode for small metallic spheres. If the particles are irregularly shaped and/or the system of particles is not dilute, the spectral function can be expected to broaden into a continuous function of n, and the peak in $\mathrm{Im}[\epsilon_m^{(1)}(\omega)]$ is correspondingly broad; one can say that the surface mode spectrum becomes continuous. The variable n can be considered as a "depolarization factor," and $G_1(n)$ is the distribution of depolarization factors associated with the geometrical shape of the regions occupied by component 1.

Consider a general composite in which component 1 is in a connected region. If component 1 is a conductor with dc conductivity σ_1 and component 2 is an insulator, then the composite will have a nonzero dc conductivity $\sigma_m^{(1)}$. We shall show later that the percolation strength C_1 is related to the ratio of these dc conductivities:

$$f_1C_1=\sigma_m^{(1)}/\sigma_1 . \tag{2.7}$$

C_1 can be considered as the fraction of component 1 that contributes to dc conductivity; i.e., isolated regions, dead ends, or a tortuous conducting path in component 1 tend to decrease C_1.

The term $C_1(\epsilon_1/\epsilon_2-1)$ in Eq. (2.5) could be obtained by replacing $G_1(n)$ by $G_1(n)+C_1\delta(n)$ and extending the range of integration so as to include the point $n=0$. From this point of view, the existence of percolation is equivalent to a special surface mode at $n=0$, which we can denote as the "percolation mode." C_1 can then be considered as the "strength of the percolation mode." We assume that $C_1=0$ in our specific system.

Similarly, the percolation strength C_2 is related to the dc conductivity of a composite in which component 2 is a conductor and component 1 is an insulator, and $G_2(n)$ is related to the surface-mode spectrum. In our specific system, $C_2>0$.

Since Eqs. (2.5) and (2.6) are alternative representations for the same composite, $G_1(n)$ and $G_2(n)$ are not independent, but are related by

$$f_1nG_1(n)=f_2(1-n)G_2(1-n) . \tag{2.8}$$

There are also sum rules, for a space with Euclidean dimension d,

$$C_1+\int_0^1 G_1(n)dn=1 , \tag{2.9}$$

$$\int_0^1 nG_1(n)dn=(1-f_1)/d , \tag{2.10}$$

with analogous expressions involving C_2, $G_2(n)$, and f_2. A third sum rule which involves both percolation strengths is

$$f_1C_1+f_2C_2+f_2\int_0^1\frac{G_2(n)}{1-n}dn=1 . \tag{2.11}$$

If the mixture function (2.1) is known explicitly, the percolation strengths and spectral functions can be determined.[17,18,35] For example, consider Eq. (2.5), which contains C_1 and $G_1(n)$. To find C_1, let $\epsilon_1\to\infty$, while ϵ_2 remains finite. Then the integral in Eq. (2.5) can be neglected, and if $C_1>0$, $\epsilon_m^{(1)}\to\infty$. Equation (2.5) then reduces to

$$f_1C_1=\lim_{\epsilon_1\to\infty}(\epsilon_m^{(1)}/\epsilon_1) . \tag{2.12}$$

The right-hand side of Eq. (2.12) can be found directly from Eq. (2.1). In the $\omega\to0$ limit, one can write $\epsilon_1=\epsilon_1'+(4\pi i/\omega)\sigma_1$ and $\epsilon_m^{(1)}=\epsilon_m'+(4\pi i/\omega)\sigma_m^{(1)}$, where σ_1 and $\sigma_m^{(1)}$ are the dc conductivities of component 1 and the composite, respectively. Then $\lim_{\epsilon_1\to\infty}(\epsilon_m^{(1)}/\epsilon_1)=\sigma_m^{(1)}/\sigma_1$, and so Eq. (2.12) is equivalent to Eq. (2.7).

In order to find $G_1(n)$, replace the integration variable n in Eq. (2.5) by n', substitute $(\epsilon_1/\epsilon_2-1)^{-1}=-(n+is)$, where $0<n<1$ and $s>0$, let $s\to0$, and take the imaginary part of the equation. One gets

$$G_1(n)=(\pi f_1)^{-1}\lim_{s\to0}\mathrm{Im}(\epsilon_m^{(1)}/\epsilon_2-1) , \tag{2.13}$$

where $(\epsilon_m^{(1)}/\epsilon_2-1)$ must be expressed as a function of $(n+is)$ by making the above substitution in Eq. (2.1).

Similarly, C_2 and $G_2(n)$ are given by

$$f_2C_2=\lim_{\epsilon_2\to\infty}(\epsilon_m^{(1)}/\epsilon_2)=\sigma_m^{(1)}/\sigma_2 , \tag{2.14}$$

$$G_2(n)=(\pi f_2)^{-1}\lim_{s\to0}\mathrm{Im}(\epsilon_m^{(1)}/\epsilon_1-1) , \tag{2.15}$$

where $(\epsilon_m^{(1)}/\epsilon_1-1)$ must be expressed as a function of $(n+is)$ by making the substitution $(\epsilon_2/\epsilon_1-1)^{-1}=-(n+is)$ in Eq. (2.1).

III. RECURSIVE CALCULATION OF SPECTRAL FUNCTION

A. Spectral representation

It will be most useful to describe the recursive relations (2.1)–(2.3) with the spectral representation in Eq. (2.6), which contains the spectral function $G_2(n)$. In particu-

lar, Eq. (2.6) is the spectral representation for the average dielectric function $\epsilon_m^{(1)}$ at the first stage [Eq. (2.1)]. For stage (j) one replaces $\epsilon_m^{(1)}$ by $\epsilon_m^{(j)}$ and ϵ_2 by $\epsilon_m^{(j-1)}$; thus the spectral representation for Eq. (2.3) is

$$\frac{\epsilon_m^{(j)}}{\epsilon_1}-1=f_2\left[C_2\left[\frac{\epsilon_m^{(j-1)}}{\epsilon_1}-1\right]+\int_0^1\frac{G_2(n)}{(\epsilon_m^{(j-1)}/\epsilon_1-1)^{-1}+n}dn\right] . \quad (3.1)$$

If the variables x and x_j, defined by

$$\epsilon_2/\epsilon_1-1=-1/x , \quad (3.2a)$$

$$\epsilon_m^{(j)}/\epsilon_1-1=-1/x_j \quad (3.2b)$$

are introduced, Eqs. (2.6) and (3.1) become

$$\frac{1}{x_1}=f_2\left[\frac{C_2}{x}+\int_0^1\frac{G_2(n)}{x-n}dn\right] , \quad (3.3)$$

$$\frac{1}{x_j}=f_2\left[\frac{C_2}{x_{j-1}}+\int_0^1\frac{G_2(n)}{x_{j-1}-n}dn\right] . \quad (3.4)$$

By defining a function

$$h(x)=\left[f_2\left[\frac{C_2}{x}+\int_0^1\frac{G_2(n)}{x-n}dn\right]\right]^{-1} , \quad (3.5)$$

Eqs. (3.3) and (3.4) can be written concisely as a recursive chain of equations:

$$x_1=h(x) , \quad (3.6a)$$

$$x_2=h(x_1)=h(h(x))\equiv h_2(x) , \quad (3.6b)$$

$$x_3=h(x_2)=h(h(h(x)))\equiv h_3(x) , \quad (3.6c)$$

$$\vdots$$

$$x_j=h(x_{j-1})\equiv h_j(x) , \quad (3.6d)$$

where we have used the notation

$$h_1(x)=h(x) ,$$
$$h_j(x)=h(h_{j-1}(x))=h_{j-1}(h(x)) . \quad (3.7)$$

Equations (3.6a)–(3.6d) show how x_j, which is related to the average dielectric function $\epsilon_m^{(j)}$ after j stages, is found by iteration, using the map $x_{j+1}=h(x_j)$, where the function h depends only on the quantities f_2, C_2, and $G_2(n)$ for the first stage.

The dielectric function $\epsilon_m^{(j)}$ at stage j must also be expressible as some function $M^{(j)}$ of the dielectric functions ϵ_1 and ϵ_2 of the two components and the actual filling fraction $\phi_2^{(j)}$:

$$\epsilon_m^{(j)}=M^{(j)}(\epsilon_1,\epsilon_2,\phi_2^{(j)}) . \quad (3.8)$$

The spectral representation of Eq. (3.8) is of the form given by Eq. (2.6), except that, on the right-hand side, we must replace f_2 by $\phi_2^{(j)}$, the actual filling fraction, C_2 by $c_2^{(j)}$, the actual percolation strength, and $G_2(n)$ by $g_2(j,n)$, the actual spectral function, at stage (j):

$$\frac{\epsilon_m^{(j)}}{\epsilon_1}-1=\phi_2^{(j)}\left[c_2^{(j)}\left[\frac{\epsilon_1}{\epsilon_2}-1\right]+\int_0^1\frac{g_2(j,n)}{(\epsilon_2/\epsilon_1-1)^{-1}+n}dn\right] . \quad (3.9)$$

If we use the variables defined by Eqs. (3.2), we can rewrite Eq. (3.9):

$$x_j=h_j(x)=\left[\phi_2^{(j)}\left[\frac{c_2^{(j)}}{x}+\int_0^1\frac{g_2(j,n)}{x-n}dn\right]\right]^{-1} . \quad (3.10)$$

The dielectric properties of the recursively constructed composite can then be described by determining how the percolation strength $c_2^{(j)}$ and spectral function $g_2(j,n)$ change as the stage index j increases, given that initially, at stage $j=1$, $c_2^{(1)}=C_2$ and $g_2(1,n)=G_2(n)$.

B. Maxwell-Garnett theory

The simplest example of the recursive procedure described in the previous section is provided by Maxwell-Garnett theory, which is discussed in Appendix A. That is, MGT is used for the mixture function M in Eqs. (2.1)–(2.3), with component 1 taken to be the spherical inclusions that are surrounded by component 2. If the mixture function for MGT is written in the form of the spectral representation (2.6), one finds for $d=3$ dimensions, at stage 1, the percolation strength $C_2=2/(2+f_1)$, whereas the spectral function consists of a single surface mode, $G_2(n)=A\delta(n-n_0)$ where $A=1-C_2$ and $n_0=1-f_2/3=(2+f_1)/3$. For example, if $f_1=0.1$, we have $n_0=0.7$ and $C_2=0.645$. Note that the function $G_2(n)$ gives the surface-mode spectrum for spherical holes of vacuum (1) surrounded by a conducting medium (2), and the depolarization factor for this surface mode approaches $n_0=\frac{2}{3}$ for low hole density $f_1\to 0$. For this geometry the spectral function $G_1(n)$, which gives the surface-mode spectrum for conducting spheres (1) surrounded by vacuum (2), is more commonly used.

The function $h(x)$, defined by Eq. (3.5), is

$$h(x)=\left[f_2\left[\frac{C_2}{x}+\frac{A}{x-n_0}\right]\right]^{-1} . \quad (3.11)$$

At stage j the iterated function $h_j(x)$ is of the form (3.10). However, the spectral function $g_2(j,n)$ is not continuous, but consists of discrete modes with strengths $a_k^{(j)}$ and depolarization factors $n_k(j)$,

$$g_2(j,n)=\sum_k a_k^{(j)}\delta(n-n_k^{(j)}) , \quad (3.12)$$

and so Eq. (3.10) becomes

$$x_j=h_j(x)=\left[\phi_2^{(j)}\left[\frac{c_2^{(j)}}{x}+\sum_k\frac{a_k^{(j)}}{x-n_k^{(j)}}\right]\right]^{-1} . \quad (3.13)$$

In order to understand how the spectral function changes as the recursions proceed, it is useful to describe a graphical method for finding the values of $n_k^{(j)}$ for the modes at stage j. For a physical composite with possibly complex dielectric functions ε_1 and ε_2, the variable x, defined by Eq. (3.2a), can be complex. In the graphical

method, we restrict x to be real and plot the function $y=h(x)$ and straight line $y=x$ in the region $0<x<1$, as shown in Fig. 2. Equation (3.11) shows that the modes at stage 1 correspond to zeros of $h(x)$, which occur at $x=0$ and $x=n_0=0.7$. The value $x=0$ is the percolation mode, and the value $x=0.7$ is the surface mode. We shall also use the notation $\{r_1\}=\{0,0.7\}$ to denote the zeros of $h(x)$ at stage 1: $h(r_1)=0$.

Similarly, Eq. (3.13) shows that, at stage j, the modes are given by the set of values $\{r_j\}$ at which $h_j(r_j)=0$. If one of the $\{r_j\}$ is zero, there is a percolation mode ($c_2^{(j)}>0$), whereas the nonzero values of $\{r_j\}$ are the depolarization factors $n_k^{(j)}$ for the surface modes.

For example, at the second stage we want to find the zeros $\{r_2\}$ of $h_2(x)$. On Fig. 2, draw a line vertically from the zero of $h(x)$ at $x=0.7$, which is point 1. This vertical line meets the line $y=x$ at the point $x=y=0.7$. A horizontal line through this point intersects the curve $y=h(x)$ at the two points (marked with the number 2) at $x=0.52$ and 0.82; these are zeros of $h_2(x)$. Similarly, starting from the zero of $h(x)$ at $x=0$, which is already on the line $y=x$, a horizontal line intersects the curve at the points $x_2=0$ and 0.7; these are also zeros of $h_2(x)$. Hence there are four zeros of $h_2(x)$, $\{r_2\}=\{0,0.7,0.52,0.82\}$; $r_2=0$ is the percolation mode, and the three nonzero values of r_2 are the depolarization factors $n_k^{(2)}$ for the surface modes. Note that the set $\{r_1\}$ is included in $\{r_2\}$.

Repeating this procedure for stage 3, we find four new values of r_3 (marked with the number 3), as well as the four values in the previous set $\{r_2\}$, giving $\{r_3\}=\{0,0.7,0.52,0.82,0.41,0.75,0.56,0.87\}$. Hence there is still a percolation mode and seven surface modes with $n_k^{(3)}>0$. At an arbitrary stage j, we find one percolation mode and 2^j-1 surface modes.

This graphical procedure can be proven algebraically. Suppose that at any stage j, r_j is a root of $h_j(x)=0$ or

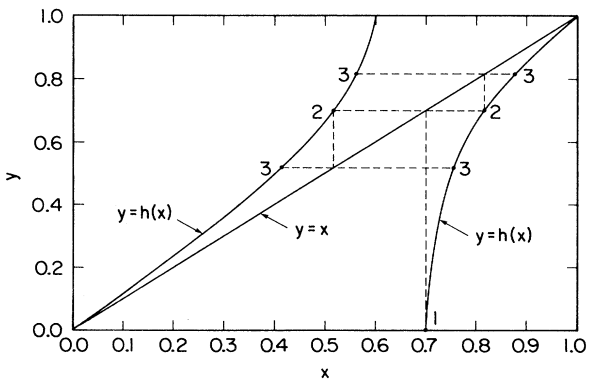

FIG. 2. Function $y=h(x)$ for the iterated MGT, given by Eq. (3.10), in $d=3$ dimensions and with initial filling factor $f_1=0.1$. A graphical method described in the text, which uses the functions $y=h(x)$ and $y=x$ to locate the positions of the new surface modes that appear in successive stages, is illustrated for the first three stages. The x values of the points marked 2 and 3 correspond to the depolarization factors $n_k^{(j)}$ of the new surface modes that appear in stages $j=2$ and 3.

$$h_j(r_j)=0\ . \tag{3.14}$$

Then the intersection of the vertical line $x=r_j$ with the line $y=x$ defines $y_j=r_j$, and the intersections of the horizontal line through this point (r_j,r_j) with $h(x)$ defines two values r_{j+1} such that $h(r_{j+1})=r_j$. Hence, from Eq. (3.7),

$$h_{j+1}(r_{j+1})=h_j(h(r_{j+1}))=h_j(r_j)$$

or, from Eq. (3.14),

$$h_{j+1}(r_{j+1})=0\ . \tag{3.15}$$

Thus r_{j+1} is a root of $h_{j+1}(x)=0$, and its value corresponds to a surface mode at stage $j+1$.

The fact that the modes $\{r_j\}$ in stage j also appear in the following stage $j+1$ is a consequence of the percolation mode; i.e., $h(0)=0$. Using Eq. (3.14), we have $h_{j+1}(r_j)=h(h_j(r_j))=h(0)=0$, which shows that r_j for stage j is indeed a zero of $h_{j+1}(x)$, the iterated function for the following stage.

The spectral function $g_2(j,n)$ at stage j could, in principle, be found by letting $x=n-is$, where $s>0$, and calculating $x_j=h_j(x)$ iteratively using Eqs. (3.6). Then Eq. (3.10) would give

$$g_2(j,n)=\frac{1}{\pi\phi_2^{(j)}}\lim_{s\to 0}\mathrm{Im}\left[\frac{1}{h_j(n-is)}\right]\ . \tag{3.16}$$

However, this procedure does not work for a numerical calculation in this case, where $g_2(j,n)$ is of the form (3.12). We must start with Eq. (3.13) and subtract the $1/x$ term (so that the percolation mode does not appear in the final result), giving a function

$$F_j(x)=\frac{1}{h_j(x)}-\frac{\phi_2^{(j)}c_2^{(j)}}{x} \tag{3.17a}$$

$$=\sum_k \frac{a_k^{(j)}}{x-n_k^{(j)}}\ . \tag{3.17b}$$

The term $\phi_2^{(j)}c_2^{(j)}/x$ in Eq. (3.17a) is known since $\phi_2^{(j)}=(\phi_2)^j$, and as will be shown in Eq. (4.15), $c_2^{(j)}=(C_2)^j$. Again, we let $x=n-is$ and take the imaginary part of Eq. (3.17), but do not go to the limit $s\to 0$. In place of Eq. (3.16), we have

$$g_2(j,n)=(\pi\phi_2^{(j)})^{-1}\mathrm{Im}F_j(x) \tag{3.18a}$$

$$=\frac{1}{\pi}\sum_k a_k^{(j)}\frac{s}{(n-n_k^{(j)})^2+s^2}\ . \tag{3.18b}$$

Hence the true spectral function (3.12) is approximated by peaks of width s and areas $a_k^{(j)}$, centered at $n=n_k^{(j)}$.

Figure 3 shows the approximate spectral functions $g_2(j,n)$ for stages $j=2$ and 3, calculated with Eqs. (3.17a) and (3.18a), as well as the stage 1 spectral function

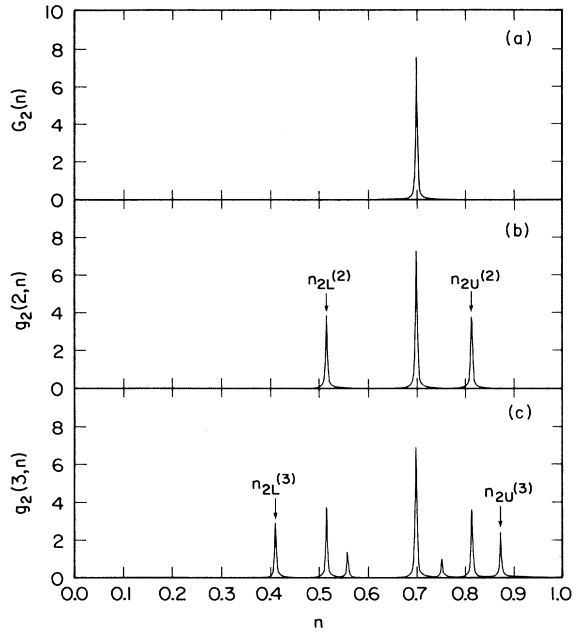

FIG. 3. Approximate spectral functions for the iterated MGT, with initial filling factor $f_1=0.1$. The value of the small parameter used to give the peaks a finite width is $s=2\times10^{-3}$. (a) Stage 1: spectral function is $G_2(n)$. (b) Stage 2: spectral function is $g_2(2,n)$. (c) Stage 3: spectral function is $g_2(3,n)$.

$g_2(1,n)\equiv G_2(n)$, whereas Fig. 4 shows $g_2(j,n)$ at stage $j=10$. From the graphical construction shown in Fig. 2, it is obvious that the mode with the smallest n value, which we denote $n_{2L}^{(j)}$, keeps moving to the left and will approach the value 0 as $j\to\infty$, and the mode with the largest n value, which we denote $n_{2U}^{(j)}$, moves to the right, approaching 1 as $j\to\infty$. These two fixed points, 0 and 1, are intersections of the line $y=x$ and the curve $y=h(x)$.

C. General spectral function

MGT for the first stage of our iterated composite system, in which the spectral function $G_2(n)$ consists of a single discrete surface mode, is actually valid only for spherical inclusions with an infinitesimally small filling fraction f_1. If the inclusions of medium 1 have irregular shapes or if f_1 is not very small, so that interactions between the randomly located inclusions become important, $G_2(n)$ will broaden into a continuous function of n.

We assume that $G_2(n)$ is different from zero only for n between a lower limit n_{2L} and an upper limit n_{2U}; i.e., $G_2(n)=0$ for $n<n_{2L}$ and $n>n_{2U}$, where $0<n_{2L}\le n_{2U}<1$. We shall call n_{2L} and n_{2U} the "takeoff" and "touchdown" limits, respectively, for $G_2(n)$. The spectral functions for the Bruggeman effective-medium theory (discussed in Appendix A), random resistor network models of composites, and of physical composites, such as porous rocks, are of this form. In MGT the takeoff and touchdown limits coincide: $n_{2L}=n_{2U}=(2+f_1)/3$.

The spectral function $g_2(j,n)$ for stage j of the recursively constructed composite can be calculated using the procedure discussed in the previous sections. We set $x=n-is$, find $h(x)$ from Eq. (3.5) [or directly from the mixture function (2.2)], and iterate $h(x)$ for any desired number of stages (j), giving $x_j=h_j(x)$. Equation (3.16) is then used to find $g_2(j,n)$.

We shall show that $n_{2L}^{(j)}$ and $n_{2U}^{(j)}$, the takeoff and touchdown limits of $g_2(j,n)$, can be located by a graphical procedure similar to that used for MGT, and that as $j\to\infty$, $n_{2L}^{(j)}\to0$ and $n_{2U}^{(j)}\to1$.

We have assumed that, at the first stage, the inclusions of medium 1 are completely surrounded by medium 2; hence $C_1=0$ and $C_2>0$. From Eq. (3.5), which defines $h(x)$, it follows that $h(0)=0$. If we set $x=1$ in Eq. (3.5) and use the sum rule (2.11), we find $h(1)=1$. Thus $x=0$ and 1 are the fixed points of the map, $x=h(x)$.

In order to visualize the graphical construction, it is convenient to imagine replacing the continuous first-stage spectral function $G_2(n)$ by a very large number of discrete surface modes separated by a very small spacing Δn,

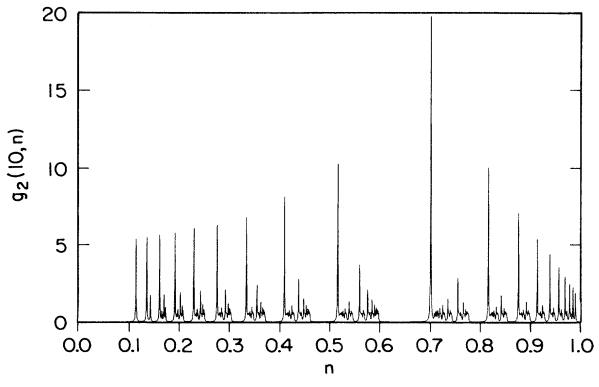

FIG. 4. Approximate spectral function $g_2(10,n)$ for stage 10 of the iterated MGT, with $f_1=0.1$ and $s=5\times10^{-4}$.

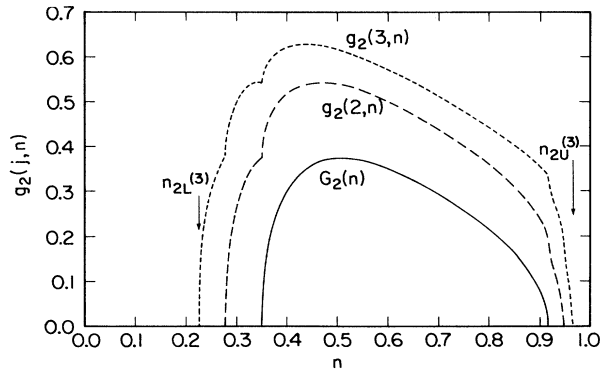

FIG. 5. Spectral functions $G_2(n)$, $g_2(2,n)$, and $g_2(3,n)$ for the first three stages of the iterated EMT, with $f_1=0.1$. The figure shows how the takeoff limit $n_{2L}^{(j)}$ moves to the left and the touchdown limit $n_{2U}^{(j)}$ moves to the right as the number of stages (j) increases.

$$G_2(n) \simeq \sum_k A_k \delta(n - n_k) , \tag{3.19}$$

where $A_k = G_2(n_k)/\Delta n$. Equation (3.5) then becomes

$$h(x) \simeq \left[f_2 \left[\frac{C_2}{x} + \sum_k \frac{A_k}{x - n_k} \right] \right]^{-1} . \tag{3.20}$$

This is similar in form to $h(x)$ for MGT [Eq. (3.11)], except that there is a closely spaced distribution of surface modes with n_k spanning the range between n_{2L} and n_{2U}, instead of a single surface mode at n_0. At stage j the spectral function $g_2(j,n)$ again consists of discrete surface modes, and so it can again be represented in the form of Eq. (3.12), giving Eq. (3.13) for x_j. The same graphical procedure which was described for MGT can again be used; the only difference is that at the first stage one begins with many closely spaced nonzero roots $\{r_1\} = \{n_k\}$ of $h(x) = 0$ instead of only one nonzero root $r_1 = n_0$. As the iteration proceeds one can follow the motion of the smallest nonzero root to the left and the largest root to the right, so that, at any stage j, the takeoff limit is $n_{2L}^{(j)} = \min\{r_j\} = \min\{n_k^{(j)}\}$, and the touchdown limit is $n_{2U}^{(j)} = \max\{r_j\} = \max\{n_k^{(j)}\}$. (The percolation mode, which corresponds to $r_j = 0$, is not considered in the above discussion.) The surface modes that appear between these takeoff and touchdown limits will be closely spaced, in contrast to the large gaps that occur between the modes when MGT is used.

In order to illustrate the procedure described above, we show in Fig. 5 the EMT spectral function $G_2(n)$ at stage 1, with initial filling fraction $f_1 = 0.1$, together with the functions $g_2(2,n)$ and $g_2(3,n)$ for the second and third stages, respectively. The takeoff and touchdown limits at stage 1 are, respectively, $n_{2L} = 0.35$ and $n_{2U} = 0.92$. At stage 2 these limits are $n_{2L}^{(2)} = 0.27$ and $n_{2U}^{(2)} = 0.95$; and at stage 3, $n_{2L}^{(3)} = 0.23$ and $n_{2U}^{(3)} = 0.97$. Figure 6 shows the function $y = h(x)$ in the regions where it is real, $0 < x < n_{2L}$ and $n_{2U} < x < 1$, together with the line $y = x$.

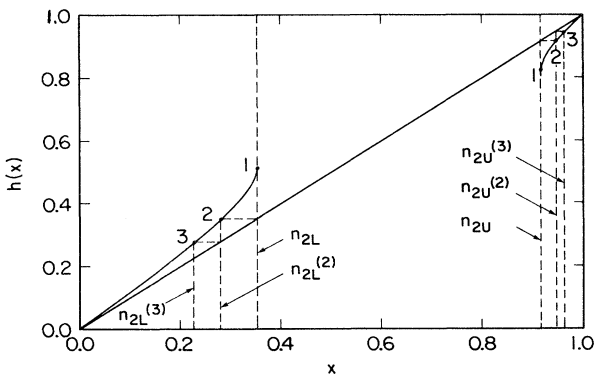

FIG. 6. Function $y = h(x)$ for the iterated EMT, in $d = 3$ dimensions, and with initial filling fraction $f_1 = 0.1$. The graphical construction described in the text is used to locate the takeoff limits $n_{2L}^{(j)}$ and the touchdown limits $n_{2U}^{(j)}$ for the first three stages.

The graphical construction used to find the takeoff limits at the three stages is shown by the dashed lines that go in vertical and horizontal steps from points $1 \to 2 \to 3$ on the left-hand side, with $n_{2L}^{(j)}$ being the abscissa of the point j. It is clear from this construction that, as one continues the iterative procedure, the points on the left side approach the fixed point $x = 0$; hence $\lim_{j \to \infty} n_{2L}^{(j)} = 0$. In a similar manner, on the right side we find the touchdown limits $n_{2U}^{(j)}$, which approach the fixed point 1 as $j \to \infty$.

IV. CRITICAL BEHAVIOR

A. Definition of critical exponents

1. Exponents t_2, s_2, and l_2

The occurrence of critical behavior in the properties of a composite in the neighborhood of a percolation threshold, as the filling fraction of the components are varied, is well known.[36–39] EMT is the simplest example of a model dielectric function which has a percolation threshold, with its associated critical behavior. The host medium 2 in our recursively constructed system also has a percolation threshold which can be approached from only one side. If component 2 is a conductor which surrounds the insulating inclusions of component 1, the system has a finite dc conductivity. As one recursively introduces more inclusions of component 1, thereby removing the conducting component 2, the dc conductivity of the composite decreases and approaches zero as the filling fraction $\phi_2^{(j)}$ of component 2 goes to zero. Hence the percolation threshold is $\phi_{2c} = 0$. However, since $\phi_2^{(j)} > 0$, one only approaches the percolation threshold as the number of iterations increases and never actually reaches the threshold or passes through it.

For this case where component 2 is a conductor and component 1 is an insulator, we define a critical exponent t_2, which describes the behavior of the dc conductivity of the composite near the percolation threshold, $\sigma_m \sim (\phi_2)^{t_2}$, or more precisely,

$$\frac{\sigma_m^{(j+1)}}{\sigma_m^{(j)}} = \left[\frac{\phi_2^{(j+1)}}{\phi_2^{(j)}} \right]^{t_2} = (f_2)^{t_2} , \tag{4.1}$$

where we have used Eq. (2.4a) to write $\phi_2^{(j+1)}/\phi_2^{(j)} = f_2$. A second critical exponent s_2 describes the behavior of the real part of the static dielectric constant, $\epsilon_m' \sim (\phi_2)^{-s_2}$, or

$$\frac{\epsilon_m'^{(j+1)}}{\epsilon_m'^{(j)}} = (f_2)^{-s_2} . \tag{4.2}$$

We are using the notation

$$\epsilon_m^{(j)} = \epsilon_m'^{(j)} + i\epsilon_m''^{(j)} = \epsilon_m'^{(j)} + 4\pi i \sigma_m^{(j)}/\omega , \tag{4.3}$$

for stage (j), in the $\omega \to 0$ (dc) limit. We have shown in the preceding section that the takeoff limit $n_{2L}^{(j)}$ for $g_2(j,n)$ approaches zero with increasing number of itera-

tions. Hence we define a third critical exponent l_2 governing the behavior of the takeoff limit, $n_{2L} \sim (\phi_2)^{l_2}$, or

$$\lim_{j\to\infty} \frac{n_{2L}^{(j+1)}}{n_{2L}^{(j)}} = (f_2)^{l_2} . \tag{4.4}$$

Since Eqs. (4.1), (4.2), and (4.4) are valid near the percolation threshold, one might expect that limit $j\to\infty$ should appear in all three equations, not just in Eq. (4.4). In Sec. IV B it will be shown that Eq. (4.1) is true for all values of j, and so the limit $j\to\infty$ is not needed here. We shall also find that $\epsilon_m'(j)$ behaves differently in two distinct large-j regions; therefore, a simple limit $j\to\infty$ in Eq. (4.2) would be misleading.

2. *Exponents t_1, s_1, and l_1*

We similarly consider the case where the inclusions of component 1 are a conductor and the surrounding component 2 is an insulator. Three critical exponents are t_1, s_1, and l_1, defined by the equations

$$\lim_{j\to\infty} \frac{\sigma_m^{(j+1)}}{\sigma_m^{(j)}} = (f_2)^{t_1} , \tag{4.5}$$

$$\lim_{j\to\infty} \frac{\epsilon_m'^{(j+1)}}{\epsilon_m'^{(j)}} = (f_2)^{-s_1} , \tag{4.6}$$

$$\lim_{j\to\infty} \frac{n_{1L}^{(j+1)}}{n_{1L}^{(j)}} = (f_2)^{l_1} . \tag{4.7}$$

Note that the takeoff limit $n_{1L}^{(j)}$ for $g_1(j,n)$ and the touchdown limit $n_{1U}^{(j)}$ for $g_2(j,n)$ are related by

$$n_{1L}^{(j)} = 1 - n_{2U}^{(j)} , \tag{4.8}$$

which follows from Eq. (2.8). Since $\lim_{j\to\infty} n_{2U}^{(j)} = 1$, we have $\lim_{j\to\infty} n_{1L}^{(j)} = 0$, showing that Eq. (4.7) is the appropriate defining equation for the critical exponent l_1 associated with the takeoff limit for $g_1(j,n)$.

B. General expressions for the critical exponents

1. *Exponents t_2, s_2, and l_2*

We begin with the case where component 2 is a conductor and component 1 is an insulator. The conductivity exponent t_2 can be found by going to the $\omega\to 0$ limit and using Eq. (4.3) for $\epsilon_m^{(j)}$ and the similar expression $\epsilon_2 = \epsilon_2' + (4\pi i/\omega)\sigma_2$ for the dielectric function of the conductor. From Eqs. (3.2a) and (3.2b), we find $x \sim i\omega/\sigma_2 \to 0$ and $x_j \sim i\omega/\sigma_m^{(j)} \to 0$, and

$$\frac{\sigma_m^{(j+1)}}{\sigma_m^{(j)}} = \frac{x_j}{x_{j+1}} . \tag{4.9}$$

In the iterative equations (3.3) and (3.4), the term containing the integral is negligible in comparison with the term containing C_2, and so we find

$$1/x_j = f_2 C_2 / x_{j-1} = \cdots = (f_2 C_2)^j / x . \tag{4.10}$$

This gives $x_j/x_{j+1} = f_2 C_2$, and Eq. (4.9) becomes

$$\sigma_m^{(j+1)}/\sigma_m^{(j)} = f_2 C_2 . \tag{4.11}$$

If we write Eq. (4.11) for the first stage ($j+1=1$), then $\sigma_m^{(j)}$ must be replaced by σ_2, giving

$$\sigma_m^{(1)}/\sigma_2 = \lim_{\omega\to 0} \epsilon_m^{(1)}/\epsilon_2 = f_2 C_2 , \tag{4.12}$$

which is the same as Eq. (2.7), with components 1 and 2 interchanged. If Eq. (4.11) is combined with Eq. (4.1), the result is

$$f_2 C_2 = (f_2)^{t_2} \tag{4.13}$$

or

$$t_2 = 1 + \frac{\ln C_2}{\ln f_2} . \tag{4.14}$$

Hence the conductivity exponent t_2 is determined by the initial filling fraction f_2 and percolation strength C_2.

The percolation strength $c_2^{(j)}$ at stage j can be found by taking the $\omega\to 0$ (or $x_j\to 0$, $x\to 0$) limit in Eq. (3.10), which becomes $1/x_j = \phi_2^{(j)} c_2^{(j)}/x$. Comparing this with Eq. (4.10), we get

$$c_2^{(j)} = (C_2)^j . \tag{4.15}$$

The exponent s_2 for the real part of the dielectric function can be found by starting with Eq. (3.1). Since component 2 is conducting, the composite system remains conducting throughout the iterative procedure. We assume that the frequency ω is not zero, but is low enough that $|\epsilon_m^{(j)}| \gg \epsilon_1$. Then the denominator of the integrand in Eq. (3.1) can be replaced by n, and Eq. (3.1), with j replaced by $j+1$, can be separated into its real and imaginary parts:

$$\frac{\epsilon_m'^{(j+1)}}{\epsilon_1} - 1 = f_2 C_2 \left[\frac{\epsilon_m'^{(j)}}{\epsilon_1} - 1 \right] + f_2 \int_0^1 \frac{G_2(n)}{n} dn . \tag{4.16a}$$

$$\epsilon_m''^{(j+1)} = f_2 C_2 \epsilon_m''^{(j)} . \tag{4.16b}$$

Equation (4.16a) gives the result that as the iteration proceeds, $\epsilon_m'^{(j)}$ approaches a fixed limit ϵ_p, which we denote as the "plateau" value. Writing $\epsilon_m'^{(j)} = \epsilon_m'^{(j+1)} = \epsilon_p$ in Eq. (4.16a), the solution for ϵ_p is

$$\epsilon_p = \epsilon_1 \left[1 + \frac{f_2}{1 - f_2 C_2} \int_0^1 \frac{G_2(n)}{n} dn \right] . \tag{4.17}$$

The evaluation of Eq. (4.17) for MGT and EMT is discussed in Appendix B.

Using Eq. (4.17), one can rewrite Eq. (4.16a) in the form

$$(\epsilon_m'^{(j+1)} - \epsilon_p)/(\epsilon_m'^{(j)} - \epsilon_p) = f_2 C_2 < 1 , \tag{4.18}$$

which shows that the difference between ϵ_m' and its limit ϵ_p becomes smaller as the number of iterations increases. Since $\epsilon_m'^{(j+1)} = \epsilon_m'^{(j)}$ for large j, it follows from the defining

equation (4.2) that

$$s_2=0 \ . \tag{4.19}$$

At a fixed (nonzero) frequency, ϵ_2' is large but finite, and so is $\epsilon_m'^{(j)}$. Equation (4.16b) shows that $\epsilon_m''^{(j)}$ becomes smaller as j increases, and so, with sufficiently many iterations, the condition $|\epsilon_m^{(j)}| \gg \epsilon_1$ for the validity of Eqs. (4.16) breaks down, and one finds that $\epsilon_m'^{(j)}$ eventually becomes smaller than ϵ_p and approaches ϵ_1. Figure 7 shows a plot of $\epsilon_m'^{(j)}$, calculated using EMT, as a function of the filling fraction $\phi_1^{(j)}$ for several values of f_1. As one follows a curve from right to left with increasing j, $\epsilon_m'^{(j)}$ first approaches the plateau value ϵ_p, but eventually approaches $\epsilon_1=1$.

The exponent l_2, which describes the approach of the takeoff limit $n_{2L}^{(j)}$ to the fixed point 0, can be found easily from the slope of the function $h(x)$ at $x=0$. One can proceed using the graphical construction shown in Fig. 6. Alternatively, using the arguments given in Sec. III, one has $h_j(n_{2L}^{(j)})=0$ and $h_{j+1}(n_{2L}^{(j+1)})=0$, from which it follows that

$$h(n_{2L}^{(j+1)})=n_{2L}^{(j)} \ . \tag{4.20}$$

We make the linear approximation, near $x=0$,

$$h(x)\simeq R_L x \ , \tag{4.21}$$

where R_L is the slope of $h(x)$ at $x=0$:

$$R_L=\left.\frac{dh}{dx}\right|_{x=0} \ . \tag{4.22}$$

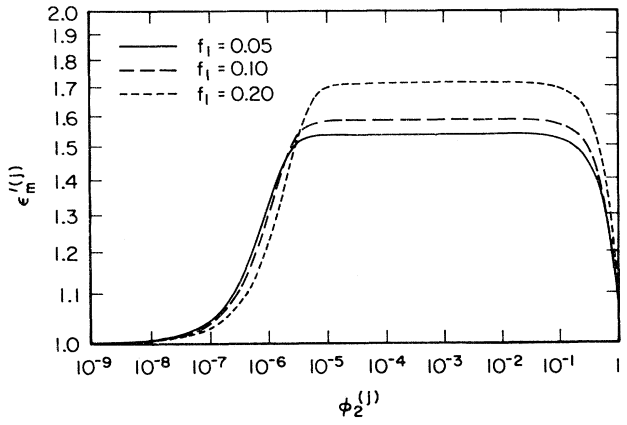

FIG. 7. Real part of the low-frequency dielectric function $\epsilon_m'^{(j)}$ against filling fraction $\phi_2^{(j)}$ of medium 2, for dimension $d=3$. The dielectric functions of the components are $\epsilon_1=1$ and $\epsilon_2=1+1.0\times10^9 i$. Three values of the initial filling fraction have been used: $f_1=0.05$, 0.10, and 0.2. The actual filling fraction $\phi_2^{(j)}=(1-f_1)^j$ takes on discrete values which decrease as the number of stages (j) increases, and so actually each curve consists of discrete points, which are not shown. The curves in the figure, which have been drawn so as to pass through these points, show how the values of $\epsilon_m'^{(j)}$ first approach a constant plateau value ϵ_p as the number of stages increases, but eventually approach the value $\epsilon_m'^{(j)}=1$ as $j\to\infty$.

Then Eq. (4.20) can be written: $R_L n_{2L}^{(j+1)}=n_{2L}^{(j)}$ or

$$n_{2L}^{(j+1)}/n_{2L}^{(j)}=1/R_L \ . \tag{4.23}$$

Using Eq. (4.23) in Eq. (4.4), we find

$$l_2=-\ln(R_L)/\ln(f_2) \ . \tag{4.24}$$

The slope R_L can be found by differentiating the function $h(x)$, defined by Eq. (3.5). The result is

$$R_L=1/(f_2C_2) \ , \tag{4.25}$$

and Eq. (4.24) gives

$$l_2=1+\frac{\ln C_2}{\ln f_2} \ . \tag{4.26}$$

2. *Exponents t_1, s_1, and l_1*

We now turn to the case where component 1 is a conductor and component 2 is an insulator. Since the insulating component 2 always surrounds the inclusions of the conducting component 1 at every stage of iteration, the dc conductivity of the composite is zero: $\sigma_m^{(j)}=0$. Hence, from Eq. (4.4), we have

$$t_1=0 \ . \tag{4.27}$$

To find s_1 it is convenient to write the iterative procedure for going from stage j to stage $j+1$ using the spectral function $G_1(n)$. Equation (2.5), with $C_1=0$, gives ϵ_m^1 at stage 1. The equation which takes us from stage j to stage $j+1$ is found by replacing $\epsilon_m^{(1)}\to\epsilon_m^{(j+1)}$ and $\epsilon_2\to\epsilon_m^{(j)}$ in Eq. (2.5):

$$\frac{\epsilon_m^{(j+1)}}{\epsilon_m^{(j)}}=1+f_1\int_0^1\frac{G_1(n)}{(\epsilon_1/\epsilon_m^{(j)}-1)^{-1}+n}dn \ . \tag{4.28}$$

Since component 1 is conductor, $|\epsilon_1|\to\infty$ in the $\omega\to0$ limit, and so the term $(\epsilon_1/\epsilon_m^{(j)}-1)^{-1}$ in the denominator of the integrand in Eq. (4.28) can be dropped, giving the ratio of static dielectric constants,

$$\epsilon_m'^{(j+1)}/\epsilon_m'^{(j)}=R_U \ , \tag{4.29}$$

where

$$R_U=1+f_1\int_0^1\frac{G_1(n)}{n}dn \ . \tag{4.30}$$

Using Eq. (4.29) in Eq. (4.6), which defines s_1, we get

$$s_1=-\ln(R_U)/\ln(f_2) \ . \tag{4.31}$$

The actual value of $\epsilon_m'^{(j+1)}$ can be found by using Eq. (2.5), which gives $\epsilon_m^{(1)}=R_U\epsilon_2$ at the first stage, together with Eq. (4.29). The result is

$$\epsilon_m'^{(j)}=(R_U)^j\epsilon_2 \ , \tag{4.32}$$

which clearly shows how the static dielectric constant of the composite can reach very large values, since it is multiplied by the factor $R_U>1$ at each stage of iteration.

The third critical exponent l_1, defined by Eq. (4.7), is

found by first noting the relation (4.8) between the takeoff limit $n_{1L}^{(j)}$ for $g_1(j,n)$ and the touchdown limit $n_{2U}^{(j)}$ for $g_2(j,n)$. We have

$$\frac{n_{1L}^{(j+1)}}{n_{1L}^{(j)}}=\frac{1-n_{2U}^{(j+1)}}{1-n_{2U}^{(j)}} , \tag{4.33}$$

which we can find by following the touchdown limit $n_{2U}^{(j)}$ for $g_2(j,n)$ in Fig. 6 as it moves to the right toward the fixed point $x=1$. A linear approximation to $h(x)$ near $x=1$ gives

$$\frac{1-h(x)}{1-x}\simeq\left.\frac{dh}{dx}\right|_{x=1} . \tag{4.34}$$

If we let $x=n_{2U}^{(j+1)}$ and note that $h(x)=h(n_{2U}^{(j+1)})=n_{2U}^{(j)}$, Eq. (4.34) becomes

$$\frac{1-n_{2U}^{(j)}}{1-n_{2U}^{(j+1)}}=\left.\frac{dh}{dx}\right|_{x=1} . \tag{4.35}$$

By differentiating Eq. (3.5) and using $h(1)=1$, we find

$$\left.\frac{dh}{dx}\right|_{x=1}=f_2\left[C_2+\int_0^1\frac{G_2(n)}{(1-n)^2}dn\right] . \tag{4.36}$$

If we insert $(1-n)+n$ into the numerator of the integrand in Eq. (4.36), the integral can be split into two parts and the sum rule (2.11) can be used, giving the expression $1+f_2\int G_2(n)n(1-n)^{-2}dn$ for the right-hand side of Eq. (4.36). Finally, using the relation (2.8) to express the integrand in terms of $G_1(n)$, we find,

$$\left.\frac{dh}{dx}\right|_{x=1}=R_U , \tag{4.37}$$

where R_U is defined in Eq. (4.30). Combining Eqs. (4.33), (4.35), and (4.37), we find

$$n_{1L}^{(j+1)}/n_{1L}^{(j)}=1/R_U . \tag{4.38}$$

Therefore, from Eq. (4.7), the critical exponent l_1 is

$$l_1=-\ln(R_U)/\ln(f_2) . \tag{4.39}$$

We have found that $l_1=s_1$ [Eqs. (4.31) and (4.39)] and $t_1=0$, and so the critical exponents satisfy

$$l_1=s_2+t_1 . \tag{4.40a}$$

Similarly $l_2=t_2$ [Eqs. (4.14) and (4.26)] and $s_2=0$, from which it follows that

$$l_2=s_2+t_2 . \tag{4.40b}$$

The relations (4.40a) and (4.40b) are valid also for EMT, for which $l_\alpha=2$, $s_\alpha=t_\alpha=1$, $\alpha=1,2$, and as shown in Ref. 17, they are consistent with the scaling relations proposed by Bergman and Imry[37] and Stroud and Bergman.[38]

C. Values of the critical exponents

In order to find specific values of the critical exponents, we must specify the mixture function M in Eqs. (2.1)–(2.3). We shall consider only the two most well-known mixture functions: Maxwell-Garnett theory[34] and Bruggeman effective-medium theory.[33] The differential effective-medium theory, in which an infinitesimally small fraction f_1 of component 1 is added at each stage, is obtained by taking the limit $f_1\to 0$ for either MGT or EMT.

The exponents l_2 $(=t_2)$, given by Eq. (4.14), depend on the percolation strength C_2, which is given in Appendix A for MGT and EMT. In order to find l_1 $(=s_1)$, given by Eq. (4.31), we must find R_U using either Eq. (4.30) or (4.37); this is done in Appendix B.

All quantities can be expressed in terms of the Euclidean dimension d of the space and initial fraction f_1 of the inclusions of component 1 and are summarized below.

(i) Maxwell-Garnett theory:

$$l_1=s_1=-\frac{\ln[1+f_1d/(1-f_1)]}{\ln(1-f_1)} , \tag{4.41}$$

$$l_2=t_2=\frac{\ln[1-f_1d/(d-1-f_1)]}{\ln(1-f_1)} , \tag{4.42}$$

$$\epsilon_p/\epsilon_1=\frac{d}{d-1+f_1} . \tag{4.43}$$

(ii) Effective-medium theory:

$$l_1=s_1=\frac{\ln(1-f_1d)}{\ln(1-f_1)} , \tag{4.44}$$

$$l_2=t_2=\frac{\ln[1-f_1d/(d-1)]}{\ln(1-f_1)} , \tag{4.45}$$

$$\epsilon_p/\epsilon_1=\frac{d(1-f_1)}{d-1-f_1d} . \tag{4.46}$$

(iii) Differential effective-medium theory:

$$l_1=s_1=d , \tag{4.47}$$

$$l_2=t_2=\epsilon_p/\epsilon_1=d/(d-1) . \tag{4.48}$$

Table I gives values of the critical exponents and ϵ_p/ϵ_1 for MGT and EMT with two choices for f_1 (0.05 and 0.1) in dimensions $d=2$, 3, and 6.

The conductivity exponent t_2 depends on f_1 and decreases with higher d. This behavior is quite different from that of random resistor networks, where t_2 is unique for a given dimension d, independent of lattice structure, and increases with d, starting from an approximate value of 1.1–1.3 in $d=2$ and reaching an asymptotic value of 3.000 for $d\geq 6$.[20,21,24] The different dependence of t_2 on d arises because, in our system, every part of the conducting component 2 can contribute to the conductivity, whereas in a random resistor network, there are isolated clusters of conducting resistors and dead ends, which do not contribute to the conductivity.

In Fig. 8 the critical exponents and plateau values are shown as functions of the initial filling fraction f_1 in $d=3$ dimensions for both MGT and EMT. For MGT all quantities remain well behaved for all values of f_1, but for EMT, l_1 $(=s_1)$ diverges as $f_1\to\frac{1}{3}$, and l_2 $(=t_2)$ and ϵ_p/ϵ_1 diverge as $f_1\to\frac{2}{3}$. These divergences are associat-

TABLE I. Critical exponents l_1 ($=s_1$), l_2 ($=t_2$), and plateau values ϵ_p/ϵ_1 for recursively constructed composites, with initial filling factors $f_1=0.05$, and 0.1 and dimensions $d=2$, 3, and 6.

		l_1, s_1		l_2, t_2		ϵ_p/ϵ_1	
	d \ f_1	0.05	0.10	0.05	0.10	0.05	0.10
MGT	2	1.951	1.905	1.951	1.905	1.905	1.818
	3	2.858	2.730	1.481	1.463	1.463	1.428
	6	5.350	4.848	1.194	1.188	1.188	1.176
EMT	2	2.054	2.118	2.054	2.118	2.111	2.250
	3	3.168	3.385	1.520	1.542	1.540	1.588
	6	6.954	8.700	1.206	1.213	1.213	1.227

ed with percolation thresholds that occur in EMT.

MGT can formally be used for any $f_1<1$, since component 1 never percolates. However, this is not true for EMT, in which there is a percolation threshold for component 1 at $f_1=f_{1c}=1/d=\frac{1}{3}$. If $f_1\to\frac{1}{3}$, then $n_{1L}\to 0$, and so the touchdown limit for $G_2(n)$ $n_{2U}=1-n_{1L}\to 1$. In Fig. 6 the entire right-hand branch of the function $h(x)$ for $n_{2U}<x<1$ disappears at the percolation threshold. Therefore, the critical exponents l_1 and s_1, which are related to the way in which $n_{2U}^{(j)}$ approaches 1 with increasing j, diverge as $f_1\to\frac{1}{3}$.

The critical exponents l_2 and t_2 are not affected by the percolation threshold for component 1 at $f_1=f_{1c}$ in EMT, and so our assumption that component 1 does not percolate has no significance for these critical exponents. However, there is a percolation threshold for component 2 at $f_2=f_{2c}=1/d$ or $f_1=1-f_{2c}=(d-1)/d=\frac{2}{3}$, which is where l_2 ($=t_2$) and ϵ_p/ϵ_1 diverge. In Fig. 6 the entire left-hand branch of $h(x)$ for $0<x<n_{2L}$ disappears when $f_1\to\frac{2}{3}$ since $n_{2L}\to 0$; this accounts for the divergence of l_2 ($=t_2$). Even at the first stage, $\epsilon_m'^{(1)}$ diverges at the percolation threshold for the conducting component 2; this divergence also occurs for the iterated value $\epsilon_m'^{(j)}$ at stage j and, hence, for the plateau value ϵ_p.

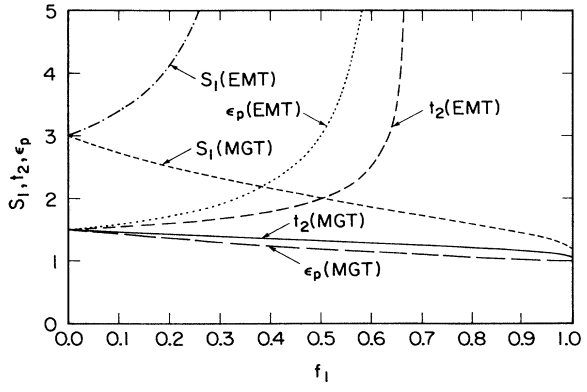

FIG. 8. Critical exponents s_1 and t_2 and plateau value ϵ_p, in $d=3$ dimensions, for both MGT and EMT, as functions of f_1. In EMT, s_1 diverges as $f_1\to\frac{1}{3}$, whereas t_2 and ϵ_p diverge as $f_1\to\frac{2}{3}$.

V. DISCUSSION

We have shown that a recursively constructed system exhibits critical behavior and have obtained general expressions for the critical exponents. We will not give an extensive discussion of applications of the theory, but will indicate briefly how it can be used to describe some properties of brine-filled porous rocks.

In brine-filled porous rocks, both the pore space, which is filled with brine (the conducting component), and the rock (the insulating component) must form connected (percolating) regions. There also should be no isolated regions of pore space; otherwise, it would be impossible to fill all of this space with brine. The mechanical strength of the rock implies finite areas of contact between the rock grains. Therefore, the insulating component also percolates, and also there should be no isolated regions of this component.

In our recursively constructed system, it has been assumed that only component 2 percolates, and so the theory cannot be applied immediately to porous rocks. However, the theory can be modified in order to give a system in which both components 1 and 2 percolate.

One way to modify the theory is to let component 1 be the conductor (brine) and go to any desired stage of the recursive construction, adding inclusions of component 1, just as before. A final additional step is to mix this composite, in which component 1 does not percolate, with a second composite in which component 1 percolates, using an appropriate mixture function which retains the percolation of component 1. A similar procedure is used by Claro and Brouers[40] to explain the very high static dielectric constant of certain brine-filled porous rocks. They obtain a medium (A) with a very high static dielectric constant by using a chain of very close conducting spheres of brine (component 1) in a matrix of rock (component 2). Since the brine component does not percolate, the dc conductivity of this mixture is zero. The final step is to mix this medium (A) with a conducting medium (B), having a dielectric function similar to that of brine, using MGT in which medium (B) surrounds inclusions of medium (A). The final composite has both a high static dielectric constant (from medium A) and nonvanishing dc conductivity (from medium B). Our recursive construction could be used in a similar way to obtain a medium (A) with a high static dielectric constant by recursively placing conducting spheres (component 1) into a rock host.

A second application of the theory is to derive Archie's law for the dc conductivity of brine filled porous rocks, $\sigma_m \sim \sigma_b \phi^t$, where ϕ is the porosity (the filling fraction of brine) and the exponent t is on the order of 2. Since the system is conducting for an arbitrarily small brine-filling fraction, it appears as if one could use our recursive theory with component 2 as the conducting brine ($\sigma_2 = \sigma_b$) and component 1 as the rock. The exponent t in Archie's law is the same as the conductivity exponent t_2 in our theory.

As we stated previously, the problem with this approach is that the rock component 1 does not percolate. A solution to this problem, proposed by Sheng,[7] is to initially use a mixture of rock and brine, instead of pure brine, as medium 2. If the rock in this initial mixture has filling factor $f_1^{(0)}$, the rock can be made percolating by using EMT with $f_1^{(0)} > \frac{1}{3}$. Then, when inclusions of pure rock are recursively introduced with filling factor f_1, the actual filling factor of brine at stage j will be

$$\phi_2^{(j)} = f_2^{(0)} (f_2)^j , \tag{5.1}$$

in place of Eq. (2.4a). The rock component will always remain percolating because of its presence in medium 2. Following reasoning similar to that which led to Eqs. (4.10)–(4.12), the dc conductivity at stage j is

$$\sigma_m^{(j)} = \sigma_2 f_2^{(0)} C_2^{(0)} (f_2 C_2)^j , \tag{5.2}$$

where $C_2^{(0)}$ is percolation strength of the rock in the initial mixture. Taking the ratios of Eqs. (5.1) and (5.2) for successive stages, we arrive at Eq. (4.12) for the conductivity ratio and Eq. (4.14) for the conductivity exponent t_2, just as before.

If one uses EMT with $f_1 = f_2 = 0.5$ for the recursive construction, Eq. (4.45) gives $t_2 = 2$, which is the desired result. However, the filling factor $\phi_2^{(j)}$ of rock becomes small very rapidly as the number of stages increases, and so it may be difficult to reach a specific value of ϕ_2. Sheng used DEMT by going to the limit $f_1 \to 0$ and letting the number of stages $j \to \infty$, making it easy to reach any desired value of $\phi_2^{(j)}$. However, our DEMT result in Eq. (4.48), which was derived from the simplest MGT (or EMT) with spherical inclusions of rock, gives $t_2 = 1.5$, which is too small. If one uses ellipsoidal inclusions, any desired value of t_2 can be obtained. The spectral function $G_2(n)$ for ellipsoidal inclusions with depolarization factors n_a, n_b, and n_c, in the limit $f_1 \to 0$, is

$$G_2(n) = [\delta(n - n_a) + \delta(n - n_b) + \delta(n - n_c)]/3 , \tag{5.3}$$

where $n_a + n_b + n_c = 1$. If we use this spectral function in Eq. (2.5) and go to the limit $\epsilon_2 \to \infty$ and $\epsilon_m^{(1)} \to \infty$, we find an expression for $\epsilon_m^{(1)}/\epsilon_2$. Then Eq. (2.6) immediately gives

$$f_2 C_2 = \epsilon_m^{(1)}/\epsilon_2 = 1 - \frac{f_1}{3} \sum_i \frac{1}{1 - n_i} . \tag{5.4}$$

From Eq. (4.14), taking the limit $f_1 \to 0$, we find the conductivity exponent

$$t_2 = \frac{1}{3} \sum_i \frac{1}{1 - n_i} . \tag{5.5}$$

For a spheroidal shape, we take $n_c = n_\parallel$ and $n_a = n_b = (1 - n_\parallel)/2$, giving

$$t_2 = \frac{1}{3} \left[\frac{5 - 3n_\parallel^2}{1 - n_\parallel^2} \right] , \tag{5.6}$$

a result also found by Sheng.[7]

The value $n_\parallel = 0.73$, which corresponds to a prolate spheroid, gives the desired result, $t_2 = 2$. It is clear from Eq. (5.5) that t_2 can attain large values if any depolarization factor approaches 1, which corresponds to very flat pancake-shaped ellipsoidal inclusions of rock. Values of t_2 as high as 4 have, in fact, been measured in some rocks.

We have pointed out the values of l_2 ($= t_2$) and s_2 do not depend on whether or not component 1 percolates, since these exponents depend on the way in which the takeoff limit $n_{2L}^{(j)}$ approaches the fixed point $x = 0$ of $h(x)$. However, our assumption that component 1 does not percolate ($C_1 = 0$) is important in the determination of l_1 ($= s_1$), since these exponents depend on the approach of the touchdown limit $n_{2L}^{(j)}$ toward the fixed point $x = 1$ of $h(x)$. If $C_1 > 0$, the fixed point of $h(x)$ is $x < 1$, and therefore Eqs. (4.39) for l_1 and (4.31) for s_1 become invalid. In future work the theory will be extended to the case $C_1 > 0$. It will also be of interest to study the frequency-dependent dielectric properties.

ACKNOWLEDGMENTS

We thank Francisco Claro for many helpful discussions. The Ames Laboratory is operated for the U.S. Department of Energy by Iowa State University under Contract No. W-7405-Eng-82. Part of this work was performed at Jackson State University within the Lawrence Berkeley Laboratory/Jackson State University/Ana G. Mendez Educational Foundation Science Consortium under U.S. Department of Energy, Office of Energy Research, Contract No. DE-FG 05-86ER75274.

APPENDIX A

For convenience, we present well-known results for Maxwell-Garnett theory and effective-medium theory. The Euclidean dimension of the space is d.

1. MGT

The equation for the average dielectric function $\epsilon_m^{(1)}$ for spherical inclusions with dielectric function ϵ_1 and filling fraction f_1, surrounded by a host with dielectric function ϵ_2, is

$$\frac{\epsilon_m^{(1)} - \epsilon_2}{\epsilon_m^{(1)} + (d-1)\epsilon_2} = f_1 \frac{\epsilon_1 - \epsilon_2}{\epsilon_1 + (d-1)\epsilon_2} . \tag{A1}$$

To find C_2 and $G_2(n)$, it is easier to use an alternate procedure instead of Eqs. (2.14) and (2.15). Defining variables x and x_1 by Eqs. (3.2), we can rewrite Eq. (A1) as

$$\frac{1}{x_1}=f_2\left[\left[\frac{d-1}{d-f_2}\right]\frac{1}{x}+\left[\frac{1-f_2}{d-f_2}\right]\frac{1}{x-(1-f_2/d)}\right] . \tag{A2}$$

Comparison of Eq. (A2) with Eq. (3.3) gives

$$C_2=(d-1)/(d-f_2) , \tag{A3}$$

$$G_2(n)=A\delta(n-n_0) , \tag{A4}$$

with $A=(1-f_2)/(d-f_2)=1-C_2$ and $n_0=1-f_2/d$.

2. EMT

The equation for the average dielectric function $\epsilon_m^{(1)}$ is

$$f_1\frac{\epsilon_1-\epsilon_m^{(1)}}{\epsilon_1+(d-1)\epsilon_m^{(1)}}+f_2\frac{\epsilon_2-\epsilon_m^{(1)}}{\epsilon_2+(d-1)\epsilon_m^{(1)}}=0 . \tag{A5}$$

This is a quadratic equation for $\epsilon_m^{(1)}/\epsilon_1$, with the solution

$$\frac{\epsilon_m^{(1)}}{\epsilon_1}=\frac{b\pm[b^2+4(d-1)\epsilon_2/\epsilon_1]^{1/2}}{2(d-1)} , \tag{A6}$$

where

$$b=f_1d-1+(d-1-f_1d)\epsilon_2/\epsilon_1 . \tag{A7}$$

The percolation strength C_2, which can be found directly from Eq. (A5) using Eq. (2.14), is

$$C_2=\begin{cases}\dfrac{f_2d-1}{f_2(d-1)}, & f_2>\dfrac{1}{d}\\ 0, & f_2<\dfrac{1}{d}\end{cases} . \tag{A8}$$

The spectral function $G_2(n)$ is found from Eqs. (A7) and (2.15):

$$G_2(n)=\begin{cases}\left[\dfrac{d}{2\pi(d-1)f_2}\right]\dfrac{[(n-n_{2L})(n_{2U}-n)]^{1/2}}{n}, & n_{2L}<n<n_{2U}\\ 0, & n<n_{2L},\ n>n_{2U} ,\end{cases} \tag{A9}$$

where

$$\left.\begin{matrix}n_{2L}\\ n_{2U}\end{matrix}\right\}=k\pm(k-\Delta)^{1/2}(k+\Delta)^{1/2} , \tag{A10}$$

with

$$k=[2(d-1)+d(d-2)\Delta]/d^2 , \tag{A11}$$

$$\Delta=f_2-1/d . \tag{A12}$$

APPENDIX B

1. Determination of plateau value ϵ_p

The general equation (4.17) for ϵ_p depends on the integral $\int n^{-1}G_2(n)dn$, which we must evaluate for both MGT and EMT. The evaluation is simple for MGT, since $G_2(n)$ consists of a Dirac δ function [Eq. (A4)]. Inserting Eq. (A4) for $G_2(n)$ and Eq. (A3) for C_2 into Eq. (4.17), we arrive at Eq. (4.43) for ϵ_p/ϵ_1.

For EMT it is possible to evaluate the integral by using the explicit function $G_2(n)$ given in Eq. (A9). However, it is easier to use a series expansion method to find the integral. We introduce the variable x, defined in Eq. (3.2a), into Eq. (3.1), which becomes

$$\frac{\epsilon_m^{(1)}}{\epsilon_1}-1=f_2\left[-\frac{C_2}{x}+\int_0^1\frac{G_2(n)}{n-x}dn\right] . \tag{B1}$$

Expanding $(n-x)^{-1}$ as a power series in x, we can write Eq. (B1) as

$$\frac{\epsilon_m^{(1)}}{\epsilon_1}-1=-\frac{f_2C_2}{x}+f_2\int_0^1\frac{G_2(n)}{n}dn+f_2x\int_0^1\frac{G_2(n)}{n^2}dn+\cdots . \tag{B2}$$

If the right-hand side of Eq. (A6), which is an explicit expression for $\epsilon_m^{(j)}/\epsilon_1$, is expressed in terms of x and expanded in a power series, we find a result of the form

$$\epsilon_m^{(1)}/\epsilon_1-1=a_{-1}x^{-1}+a_0+a_1x+a_2x^2+\cdots . \tag{B3}$$

The positive sign in front of the square root in Eq. (A6) must be taken to calculate this power series, which is a small-x expansion. Equating coefficients of corresponding powers of x in Eqs. (B2) and (B3), we find

$$f_2C_2=-a_{-1} , \tag{B4}$$

$$f_2\int_0^1\frac{G_2(n)}{n}dn=a_0 . \tag{B5}$$

Equation (B4) gives a result for C_2 which agrees with Eq. (A8), whereas Eq. (B5) gives

$$f_2\int_0^1\frac{G_2(n)}{n}dn=\frac{d(1-f_2)}{(d-1)(f_2d-1)} , \tag{B6}$$

which we use in Eq. (4.17) to give Eq. (4.46) for ϵ_p/ϵ_1.

2. Determination of R_U

The quantity R_U, which is used in the calculation of the critical exponent s_1 $(=l_1)$, can be calculated using any of the equivalent equations (4.30), (4.36), or (4.37). For MGT it is easiest to use Eq. (4.30), with the spectral function $G_1(n)=\delta(n-n_0')$, where $n_0'=(1-f_1)/d$, to give

$$R_U=1+f_1d/(1-f_1) . \tag{B7}$$

For EMT it is easiest to use Eq. (4.37), in which dh/dx must be evaluated at $x=1$. We can find $h(x)$ by starting with Eq. (A6), introducing the variables x_1 and x defined by Eqs. (3.2) and using the definition (3.5) for $h(x)$. The result is

$$x_1 = h(x) = \left[1 - \frac{b - [b^2 + 4(d-1)(1-1/x)]^{1/2}}{2(d-1)}\right]^{-1}, \quad \text{(B8)}$$

where

$$b = (f_1 d - 1) + (d - 1 - f_1 d)(1 - 1/x) . \quad \text{(B9)}$$

In order to give the correct result $h(1)=1$, we have used a negative sign in front of the square root in Eq. (B8). By direct differentiation we find

$$R_U = \left.\frac{dh}{dx}\right|_{x=1} = (1 - f_1 d)^{-1} . \quad \text{(B10)}$$

[1] R. Landauer, in *Electrical Transport and Optical Properties of Inhomogeneous Media,* Proceedings of the First Conference on the Electrical Transport and Optical Properties of Inhomogeneous Media, edited by J. C. Garland and D. B. Tanner, AIP Conf. Proc. No. 40 (AIP, New York, 1978), p. 2.

[2] P. N. Sen, C. Scala, and M. H. Cohen, Geophysics **46**, 781 (1981).

[3] P. M. Sen, Geophysics **46**, 1714 (1981).

[4] K. S. Mendelson and M. H. Cohen, Geophysics **47**, 257 (1981).

[5] P. N. Sen, Geophysics **49**, 586 (1984).

[6] P. Sheng and A. J. Callegari, in *Physics and Chemistry of Porous Media,* Proceedings of a Symposium on the Physics and Chemistry of Porous Media, edited by D. L. Johnson and P. N. Sen, AIP Conf. Proc. No. 107 (AIP, New York, 1984), p. 144.

[7] P. Sheng, Phys. Rev. B **41**, 4507 (1990).

[8] P. C. Lysne, Geophysics **48**, 775 (1983).

[9] J. Korringa, Geophysics **49**, 1760 (1984).

[10] B. I. Halperin, S. Feng, and P. N. Sen, Phys. Rev. Lett. **54**, 2391 (1985).

[11] P. N. Sen, J. N. Roberts, and B. I. Halperin, in *Percolation Structures and Processes* (Ref. 23), p. 278.

[12] *Physics and Chemistry of Porous Media* (Ref. 6).

[13] *Physics and Chemistry of Porous Media II,* Proceedings of the Second International Symposium on the Physics and Chemistry of Porous Media, edited by J. R. Banavar, J. Koplik, and K. Winkler, AIP Conf. Proc. No. 154 (AIP, New York, 1987).

[14] D. J. Bergman, in *Electrical Transport and Optical Properties of Inhomogeneous Media* (Ref. 1), p. 46; Phys. Rep. **43**, 377 (1978).

[15] R. Fuchs, Phys. Rev. B **11**, 1732 (1975).

[16] R. Fuchs, in *Electrical Transport and Optical Properties of Inhomogeneous Media* (Ref. 1), p. 276.

[17] D. Stroud, G. W. Milton, and B. R. De, Phys. Rev. B **34**, 5145 (1986).

[18] K. Ghosh and R. Fuchs, Phys. Rev. B **38**, 5222 (1988).

[19] S. Kirkpatrick, Rev. Mod. Phys. **45**, 574 (1973).

[20] S. Kirkpatrick, in *Electrical Transport and Optical Properties of Inhomogeneous Media* (Ref. 1), p. 99.

[21] D. Stauffer, Phys. Rep. **54**, 1 (1979).

[22] D. Stauffer, *Introduction to Percolation Theory* (Taylor and Francis, Philadelphia, 1985).

[23] *Percolation Structures and Processes,* Vol. 5 of *Annals of the Israel Physical Society,* edited by G. Deutscher, R. Zallen, and J. Adler (Hilger, Bristol, The Israel Physical Society, Jerusalem, and AIP, New York, 1983).

[24] *Kinetics of Aggregation and Gelations,* Proceedings of the International Topical Conference on Kinetics of Aggregation and Gelation, April 2–4, 1984, Athens, Georgia, edited by F. Family and D. P. Landau (North-Holland, New York, 1984).

[25] *On Growth and Form: Fractal and Non-Fractal Patterns in Physics,* Vol. 100 of NATO Advanced Science Institute Series, Series E: Applied Sciences, edited by H. Eugene Stanley and Nicole Ostrowsky (Nijhoff, Boston, 1986).

[26] *Disordered Systems and Localization,* Proceedings of a Conference held in Rome, 1981, edited by C. Castellani, C. Di Castro, and L. Peliti, Lecture Notes in Physics, Vol. 149 (Springer-Verlag, New York, 1981).

[27] *Macroscopic Properties of Disordered Media,* Proceedings of a Conference held at the Courant Institute, 1981, edited by R. Burridge, S. Childress, and G. Papanicolaou, Lecture Notes in Physics, Vol. 154 (Springer-Verlag, New York, 1982).

[28] A. S. Skal and B. I. Shklovskii, Fiz. Tekh. Poluprovodn. **8**, 1586 (1974) [Sov. Phys. Semicond. **8**, 1029 (1975)].

[29] B. I. Shklovskii and A. L. Efros, in *Electronic Properties of Doped Semiconductors,* edited by M. Cardona, P. Fulde, and H.-J. Queisser, Springer Series in Solid-State Sciences, Vol. 40 (Springer-Verlag, New York, 1984), Chap. 5.

[30] P. G. De Gennes, J. Phys. (Paris) Lett. **72**, L1 (1976).

[31] S. Alexander and R. Orbach, J. Phys. (Paris) Lett. **43**, L625 (1982).

[32] D. Stauffer, in Ref. 22, Sec. 5.1, pp. 87–91.

[33] D. A. G. Bruggeman, Ann. Phys. (Leipzig) **24**, 636 (1935).

[34] J. C. Maxwell-Garnett, Phys. Trans. R. Soc. A **203**, 385 (1904).

[35] R. Fuchs, Phys. Rev. B **35**, 7700 (1987).

[36] A. L. Efros and B. I. Shklovskii, Phys. Status Solidi B **76**, 475 (1976).

[37] D. J. Bergman and Y. Imry, Phys. Rev. Lett. **39**, 1222 (1977).

[38] D. Stroud and D. J. Bergman, Phys. Rev. B **25**, 2061 (1982).

[39] G. Deutscher, in *Disordered Systems and Localization* (Ref. 26), p. 26.

[40] F. Claro and F. Brouers, Phys. Rev. B **40**, 3261 (1989).